American Journal of Engineering Research (AJER)
e-ISSN: 2320-0847 p-ISSN : 2320-0936
Volume-13, Issue-4, pp-76-87
www.ajer.org
Research Paper Open Access

Phase Overcurrent Relay Coordination in a Power System Network

Chukwuoko, C. J[1], Onah, A. J[2], and Diyoke, G.C[3].
Department of Electrical and Electronic Engineering,
Micheal Okpara University of Agriculture, Umudike, Abia State, Nigeria.

ABSTRACT: *It is an unsafe practice to work in a system that lacks protective coordination because in the event of short circuit fault destruction of life, property and expensive power system equipment may occur with no panacea. Short circuit faults emanating from any of three 11 kV feeders (namely, Cotgas, Ebubu and Okirika) in Refinery 15MVA, 33/11 kV injection substation either trip Bori 33KV or trip all the feeders at transmission station leaving outgoing 11kV circuit breakers uninterrupted. It is imperative to employ a well-coordinated protection scheme that will act as quickly as possible to isolate any unhealthy portion without interrupting the supply of power to healthy portions of the network. Calculation of maximum short circuit fault current (using 225MVA as base) at different buses of different voltage levels were carried out. IDMT relays (normal inverse, very inverse and extremely inverse) were used to protect the network components against short-circuit faults. MATLAB and E-TAP software were employed to coordinate the relays, showing their characteristics and various time responses during fault occurrence.*
Keywords*: Power system network, short-circuit, overcurrent, protection, relay, coordination.*

Date of Submission: 04-04-2024 Date of acceptance: 15-04-2024

I. INTRODUCTION

Phase overcurrent relay coordination is a quantitative analytical approach undertaken to ensure selectivity with high sensitivity in electrical power system network protection against overcurrent. Power system network components such as generators, transformers, motors, cables, overhead line components etc, are cost effective, and need to be protected against overcurrent. It is evident that in spite of all necessary precautions taken in the design and installation of such systems, they do encounter abnormal conditions or faults. Some of these faults are short circuits and this might be extremely damaging for not only the faulty component but for the neighbouring components (Bhuvanesh et al., 2010(a)). Overcurrent (OC) simply means excessive current in electrical circuit. Excess current is created as a result of reduced system impedance caused by short circuit between phase to phase or phase to earth of an electrical component. This excessive current generates heat that can damage electrical circuit components. Thus, it certainly needs protective devices such as fuses and circuit breakers, and over current relays for protection.

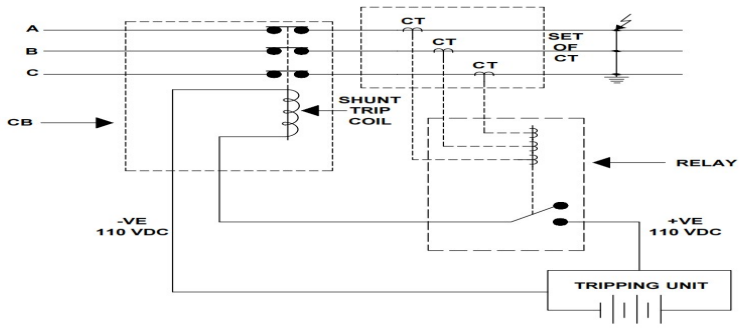

Figure 1: Description of operating procedure of a protection system.

Fig. 1 shows an over current relay contact to close the dc source for the trip coil (TC) to operate (Ram and Vishwakarma, 2011(a)). Therefore, circuit breaker (CB) is designed to interrupt/isolate normal or short circuit currents, and will automatically open a circuit whenever the line current exceeds a preset value on the relay (PHCN, 2006(a)). Fig. 1 shows that relay coil is connected to the secondary side of a set of current transformers (CT) while primary of the CT are connected to the line currents and if the line current exceeds a preset limit (threshold), secondary current will energize the relay contact to close. As soon as they are closed the shunt trip coil of the CB will be energized by an auxiliary dc source called the tripping unit and this will cause the movable contact of the CB to separate from the fixed contact, thus isolating the faulted line (Bhuvanesh et al., 2010(b)).

The aim of phase overcurrent relay coordination in a power system network is to ensure selective isolation of faulty circuits whenever there is flow of current greater than rated or current threshold on three outgoing 11KV feeders at Refinery 1 X 15MVA, 33/11KV injection substation, Portharcourt.

II. MATERIALS AND METHOD

2.1 *Single line diagram and impedance diagram*

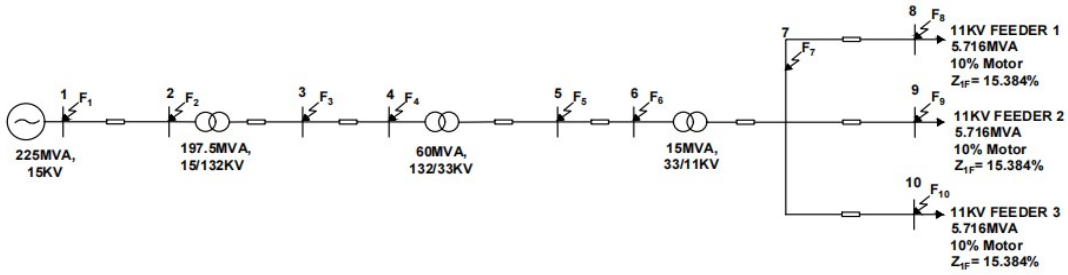

Fig. 2: Single line diagram of Refinery injection substation from the source.

The Single Line Diagram (SLD) - The Fig. 2 shows the single line diagram of the Refinery 15MVA, 33/11kV injection substation from the source (Kothari and Nagrath, 2008(a)). It is a radial network with 10 buses, 1 source gas turbine, 3 power transformers and 3 outgoing 11 kV feeders. The source of supply to Refinery 15MVA, 33/11 kV injection substation start from the gas turbine of First Independent Power Limited at Afam (known as FIPL IPP at Afam) with rated installed capacity of 225MVA, 15 kV through 197.5MVA, 15/132 kV transmission substation at the same location with FIPL IPP at Afam. The supply passed through 60MVA, 132/33 kV Transmission substation at Elelenwo to Refinery 15MVA, 33/11 kV injection substation through a 33kv circuit breaker known as Bori 33 kV feeder. The 3 outgoing 11KV feeders that radiated from the Refinery 15MVA, 33/11 kV injection substation transformer are Okirika 11 kV feeder (from bus 8), Ebubu 11 kV feeder (from bus 9) and Cot-gas 11 kV feeder (from bus 10). These three 11 kV feeders have same similar load 300A(5.716MVA at 85% power factor each) especially at peak periods.

Realization of Impedance Diagram - For maximum short circuit power (MVA_{SC}) calculation, only the positive sequence impedance of the power system components (such as generator, transformers, cables and line conductors) are employed during the calculation, the reason for non-inclusion of negative and zero sequence impedance or reactance and resistance components is that they do not flow at the occurrence of symmetrical fault (SEL, 2020).

Formulas used in calculation of per unit impedance are (Ram and Vishwakarma, 2011(b))

$$Z_1(\Omega) = \sqrt{(R^2 + X^2)} \quad (1)$$

$$Z_{1LINE}\ pu = Z(\Omega) * \frac{MVA_{base}}{KV^2} \quad (2)$$

$$Z_{1T/F}\ pu_{new} = Z_{1T/F}\ pu_{old} * \frac{MVA_{base}}{MVA_{T/F}} \quad (3)$$

Where Z_1 is positive sequence impedance, Z_{1LINE} pu is per unit positive sequence line impedance and $Z_{1T/F}$ pu is per unit positive sequence transformer impedance (Gupta, 2013).

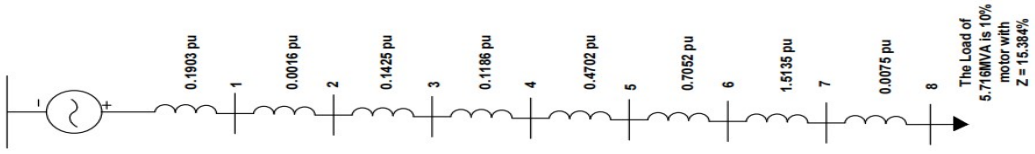

Figure. 3: The impedance diagram

Fig. 3 shows the impedance diagram (Ram and Vishwakarma, 2011(c)). The impedance values at the different buses were calculated using the technical data of generator, transformers, cables and line conductors with 225MVA (the source MVA) used as base MVA. The peak lumped load of Okirika 11 kV feeder is 300A with 10% motor and 90% static load. The peak lumped load of Ebubu 11 kV feeder is 300A with 10% motor and 90% static load. The peak lumped load of Cotgas 11 kV feeder is 300A with 10% motor and 90% static load.

2.2 ***Fault MVA and Fault current calculations***

$$\text{Fault MVA}_{SC(max)} = \frac{\text{MVA}_{\text{base}}}{Z_1 \text{ pu}_{\text{total}}} \quad (4)$$

Maximum short circuit current or Fault current becomes (Kothari and Nagrath, 2008(b));

$$\text{Fault current } I_{SC} = \frac{\text{Fault MVA}_{SC(max)}}{\sqrt{(3)} * \text{kV}_{(RATED)}} \quad (5)$$

For Bus 1,

$$\text{Fault MVA} = \frac{225}{0.1903} = 1182.34 \text{ MVA}$$

$$\text{Fault current} = \frac{1182.34}{\sqrt{3}\, x\, 15} = 45.51 \text{kA}$$

Similarly, the fault MVA and fault current are obtained for other buses

Upon fault the motor will behave as generator, introducing current into the circuit from rotor (LRC). The load on Okirirka 11KV feeder is 5.716MVA with 10% motor and Z_F = 0.15384 pu. Therefore fault current contribution from the motor becomes,

$$\text{Load Fault current } I_F \text{ contribution} = \frac{5.716 * 0.1}{0.15384 * 19.05} = 195\text{A}$$

195A will also be contributed from load on Ebubu 11 kV feeder and Cotgas 11 kV feeder because the load on these two feeders are the same with Okirika 11 kV feeder, thus the total current entering Bus 8 after fault will be,

$$I_{SC \text{ Bus } 8} = 0.195 * 2 + 3.75 = 4.14\text{kA}.$$

Likewise for Bus 9 and Bus 10 when faulted because the 3 feeders 11 kV have uniform load of 5.716MVA (10% of motor and 90% of static load) each.

2.3 ***Time and Current graded systems***

Time and Current Graded Systems - For selective operation of relay when fault occur, time graded systems disadvantage is due to the fact that the more severe faults are cleared in the longest operating time, while in current graded system, difficulty is experienced to distinguish between fault levels of two closer buses (because difference is negligible). Due to limitations encountered when using either time or current graded systems, combination of both time and current graded system has been developed. In time and current graded relays the time of operation is inversely proportional to the fault current level and the actual characteristics is a function of both time and current settings (Ram and Vishwakarma, 2011(d)). This relay characteristics function of both time and current is called inverse definite minimum time (IDMT) and it is widely used especially where grading is possible over a wide range of current with time of operation. Operation time of relays with IDMT characteristics is such that large fault currents will be interrupted more quickly and moderate operating time at low fault currents (GEYA, 2022).

The three classes of overcurrent relays are instantaneous relays, definite time relays and inverse definite minimum time relays.

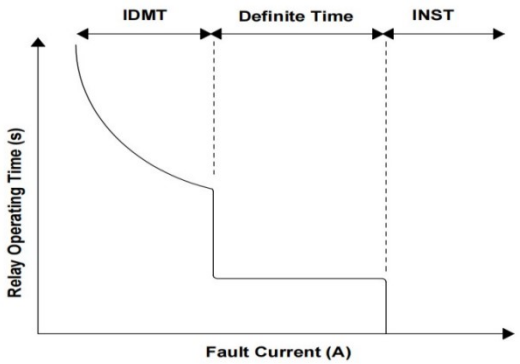

Figure 4: Time versus Fault current of IDMT relay, DT relay and Instantaneous time relay.

Instantaneous relay time of operation is zero as soon as the current value reach the threshold. The Definite time relay operating time is fixed irrespective of the fault current magnitude while inverse definite time relays (IDMT relays) are those in which their time of operations are inversely proportional to the magnitude of fault current (Electrical4u, 2019). Fig. 3 demonstrates IDMT relay, DT relay and Instantaneous time relay operating time versus fault current behaviour.

In IDMT relay characteristic curve, there is an inverse relationship for lower values of fault current while for higher values of fault current, it acts as a definite time characteristic relay.

There are four types of IDMT relays which are in compliance with either BS142/IEC or ANSI/IEEE standards and they are (Ram and Vishwakarma, 2011(e)): Normal inverse relay, Very inverse relay, Extremely inverse relay, and Long inverse relay

The general IDMT relay equation is

$$T = \frac{\beta * K}{\left(\frac{I_F}{I_S}\right)^{\alpha} - 1} \qquad (6)$$

Where

T = time of operation

$I = I_F/I_S$ = plug or pickup setting multiplier(PSM)

I_F = short circuit fault current

I_S = set current or threshold

K = time multiplier setting(TMS)

α and β = constants that will identify each of the particular IDMT relay

Table 1: Values of α and β that differentiate IDMT relays

S/N	IDMT RELAY	β	α
1	Extremely inverse	80	2.0
2	Very inverse	13.5	1.0
3	Normal inverse	0.14	0.02
4	Long inverse	120	1.0

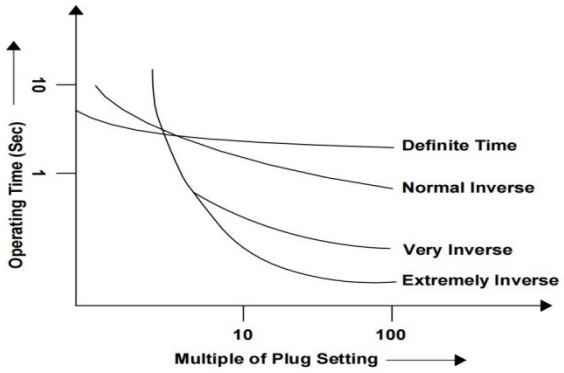

Figure 5: DT and IDMT curves

1. Normal inverse or Standard inverse

The characteristic curve of the Normal inverse or Standard inverse relay can be best described by the mathematical expression of time of operation as:

$$T = \frac{0.14 * K}{I^{0.02} - 1} \quad (7)$$

In equation 7, T is the time of operation where I_F is the fault current magnitude, I_S is the set current or threshold, K is the time multiplier setting (TMS) and I is the ratio of fault current to the threshold ($I = I_F/I_S$) known as multiple plug setting (MPS). It is best used at the source of power system for protection.

Fig. 5 shows that very inverse relay exhibits more inverse characteristics in operating time and fault current than that of Normal inverse relay. Very inverse characteristic relay curve lies between the normal inverse curve and extremely inverse curve. It is best used for protection of transmission lines. The characteristic curve can be best described by the mathematical expression of time of operation as:

$$T = \frac{13.5 * K}{I - 1} \quad (8)$$

The characteristic curve of the Extremely inverse can best be described by the mathematical expression of time of operation as:

$$T = \frac{80 * K}{I^2 - 1} \quad (9)$$

With this characteristic the operating time is approximately inversely proportional to the square of I. It is best used for feeder protection. With this characteristic the operating time is approximately inversely proportional to the magnitude of fault current (I_F).

2.4. *Phase Overcurrent Relay Coordination*

The 3 adjacent time current characteristic (TCC) relays and flow of fault current on their buses shall be analyzed (for backup purposes) (Singh, 2009). The fault current at bus 8, $I_{SC\ Bus8} = 4.14KA$,

The fault current flow at bus 7 when bus 8 is faulted will be $I_{FF\ Bus7} = 3.75$ kA (extremely inverse relay will be used as the TCC). The fault flow at bus 6 (extremely inverse relay will be used as TCC), (Murthy, 2007) the formula is,

$$V_P/V_S = I_S/I_P \quad (10)$$

$$I_{FF\ Bus\ 6} = 0.33 * 3.75 = 1.24KA$$

At bus 8 (the feeder is known as Okirika feeder), the current transformer ratio (CTR) is CT8 = 600/5A, the IDMT curve is extremely inverse, circuit breaker interruption time (T_{CB}) $T_{CB8} = 55$ms, the step delay $T_S = 0.15$ secs, the threshold setting current $I_S = 0.5I_n = 300A$ ($I_n = 600A$). From equation 9,

$T_{R8} = T_S + T_{CB8} = 0.15 + 0.055 = 0.205$ s

$$T_{R8} = \frac{80 * K_{Bus\ 8}}{\left(\frac{4140}{300}\right)^2 - 1} = 0.205 \text{ s}$$

$$K_{Bus\ 8} = K_{Bus\ 9} = K_{Bus\ 10} = 0.4854$$

This K is the same for T_{R9} and T_{R10} of Ebubu 11 kV feeder and Cotgas 11 kV feeder respectively.

At bus 7, the current transformer ratio (CTR) is 1200/5A, the IDMT curve is extremely inverse, circuit breaker interruption time (T_{CB}) $T_{CB7} = 55$ms, the step delay $T_S = 0.15$ secs, the fault current $I_{SC\ Bus7} = 3.76KA$ and the threshold setting current $I_S = 0.6I_n = 720A$ ($I_n = 1200A$). From equation 9,

$T_{R7} = T_{R8} + T_S + T_{CB\ 7} = 0.205 + 0.15 + 0.055 = 0.41$ s

$$T_{R7} = \frac{80 * K_{Bus7}}{\left(\frac{3760}{720}\right)^2 - 1} = 0.41 \text{ s}$$

$$K_{Bus7} = 0.1346$$

.Calculation for 2nd and 3rd relays in line of defense for the fault current emanating from source due to fault on any bus will depend on the magnitude of the fault flow on each bus, time current characteristic curve performance type of relay in operation and their time multiplier settings.

At bus8, $I_{SC\ BUS\ 8} = 4140A$, $T_{R8} = 0.205$ secs as already calculated but $I_{FF7} = 3750A$, $I_{FF6} = 1250A$, $I_{FF5} = 1250A$, $I_{FF4} = 313A$, therefore for operating time values,

$$T_{R7IFF8} = \frac{80 * 0.135}{\left(\frac{3750}{720}\right)^2 - 1} = 0.413 \text{ s}$$

$$T_{R6IFF8} = \frac{80 * 0.135}{\left(\frac{1250}{240}\right)^2 - 1} = 2.370 \text{ s}$$

At bus7, $I_{SC\ BUS\ 7}$ = 3760A, T_{R7} = 0.41 secs as already calculated but I_{FF6} = 1253A, I_{FF5} = 1253A, I_{FF4} = 313A, therefore for operating time values,

$$T_{R6IFF7} = \frac{80 * 0.774}{\left(\frac{1253}{240}\right)^2 - 1} = 2.358 \text{ s}$$

$$T_{R5IFF7} = \frac{13.5 * 0.208}{\left(\frac{1253}{960}\right) - 1} = 9.200 \text{ s}$$

Table 2: Summary of Relay Settings and CT Ratios

Bus	Device	IDMT	CTR	I_S (A)	TMS(K)
1	R1	SI	8000/1	7600	0.427
2	R2	SI	8000/1	7600	0.373
3	R3	SI	1000/1	840	0.224
4	R4	VI	300/1	240	0.612
5	R5	VI	1200/1	960	0.208
6	R6	EI	300/5	240	0.774
7	R7	EI	1200/5	720	0.135
8	R8	EI	600/5	300	0.485
9	R9	EI	600/5	300	0.485
10	R10	EI	600/5	300	0.485

Table 3: Summary of Fault Currents and Relay Response Time

Faults	Bus ID	I_F(KA)	T_{R8}(s)	T_{R7}(s)	T_{R6}(s)	T_{R5}(s)	T_{R4}(s)	T_{R3}(s)	T_{R2}(s)	T_{R1}(s)
F_1	1	45.51								1.639
F_2	2	45.13							1.439	1.648
F_3	3	2.94						1.237	2.105	2.410
F_4	4	2.17					1.027	1.636	2.808	-
F_5	5	4.26				0.817	2.403	6.591	-	-
F_6	6	2.42			0.615	1.846	5.433	-	-	-
F_7	7	3.76		0.410	2.358	9.200	-	-	-	-
F_8	8	4.14	0.205	0.413	2.370	-	-	-	-	-

The relay settings of R8, R9 and R10 are the same and they have the same fault current and operating time.

III. RESULTS AND DISCUSSION

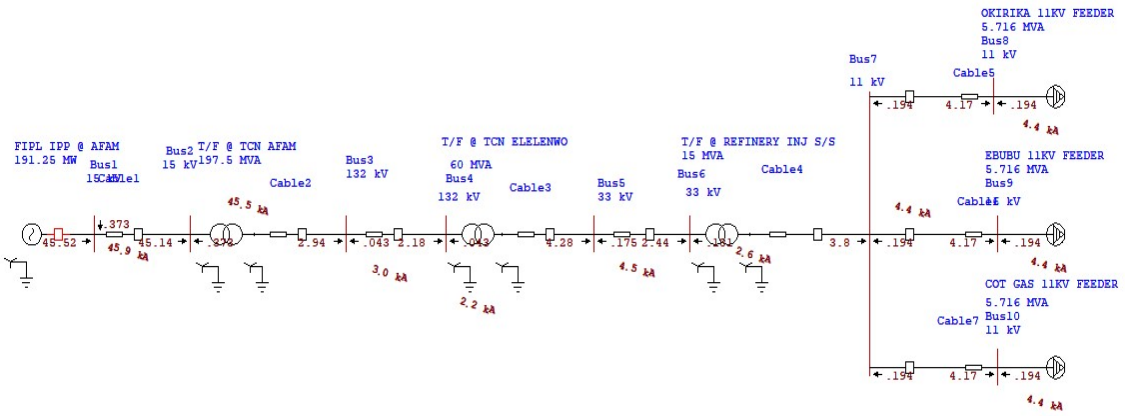

Figure 6: Result of 3-phase short circuit fault current simulation on 10 buses

Fig. 6 is the results obtained with the use of ETAP software, and it compares favourably with the summary of fault currents obtained through manual calculation as shown in Table 2.

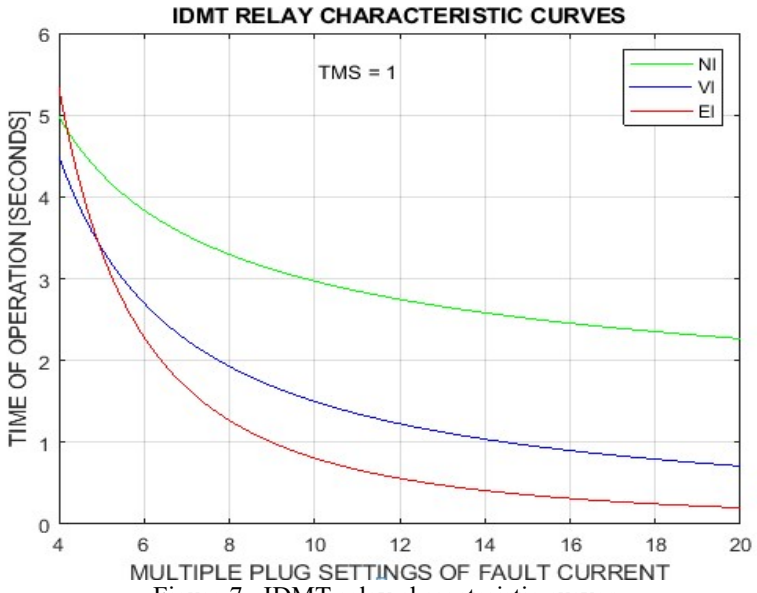

Figure 7: IDMT relay characteristic curves

As shown in Fig. 7, the Extremely inverse (EI) relay characteristic curve responds faster to high short circuit fault current than the other two curves, thus the main reason it is mostly used in feeder protection. At TMS = 1 and at multiple plug setting (MPS) of 10 this relay responds in 0.8 seconds. The Very inverse (VI) relay characteristic curve is mainly used for transmission line protection. At TMS = 1 and at multiple plug setting (MPS) of 10 this relay responds in 1.5 seconds. Normal inverse (NI) relay characteristic curve is called 3 seconds relay or 3/10 relay curve. The reason for this is that at TMS = 1 and at multiple plug setting (MPS) of 10, this relay will operate in 3 seconds, thus it is usually employed towards the source of supply for protection. According to IEC standard it is called the Normal inverse while by ANSI standard it is described as Standard inverse.

The Star Sequence-of-Operation (SQOP) software evaluates, verifies, and confirms the operations and selectivity of the protective devices for short-circuit faults in any location directly from both the single line diagram and Normalized Time Current Characteristic curve (TCC) views. The SQOP provides a realistic accurate solution for operating time of fault and specify the particular relay or any device that operated with the short circuit current value.

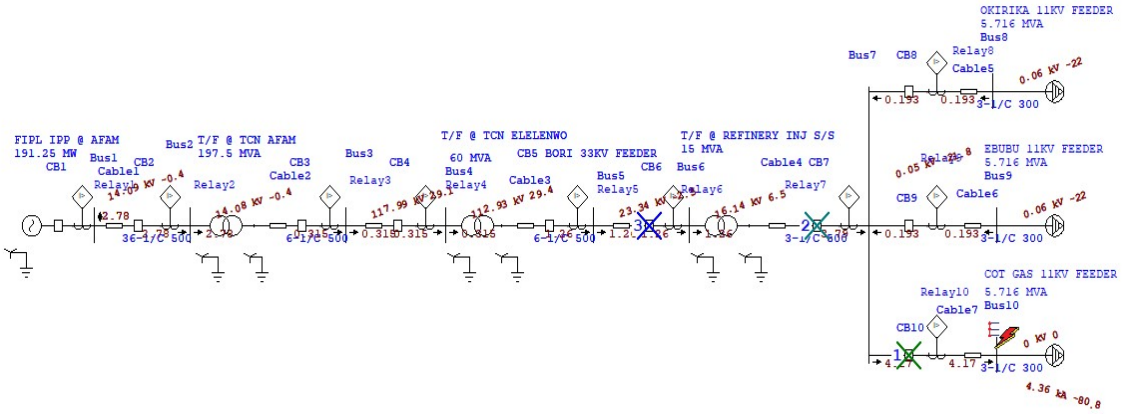

Figure 8: Star Sequence of Operation after 3-Phase Short Circuit Fault Simulation of Bus 10

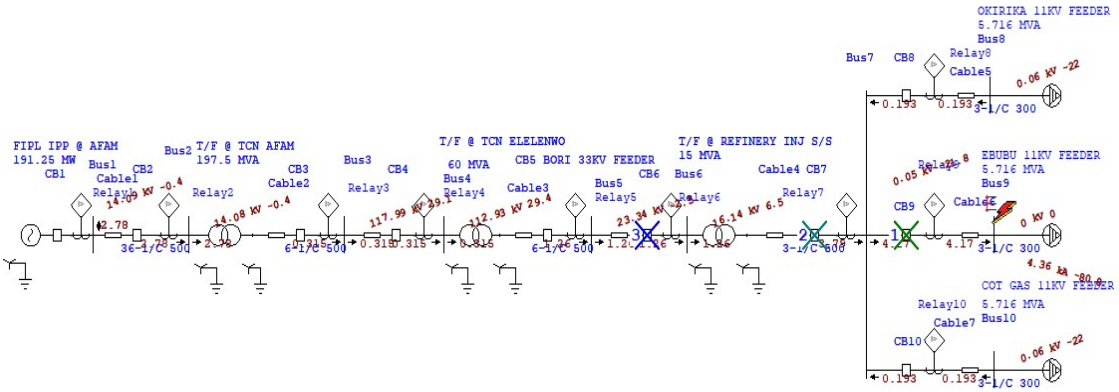

Figure 9: Star Sequence of Operation after 3-Phase Short Circuit Fault Simulation of Bus 9

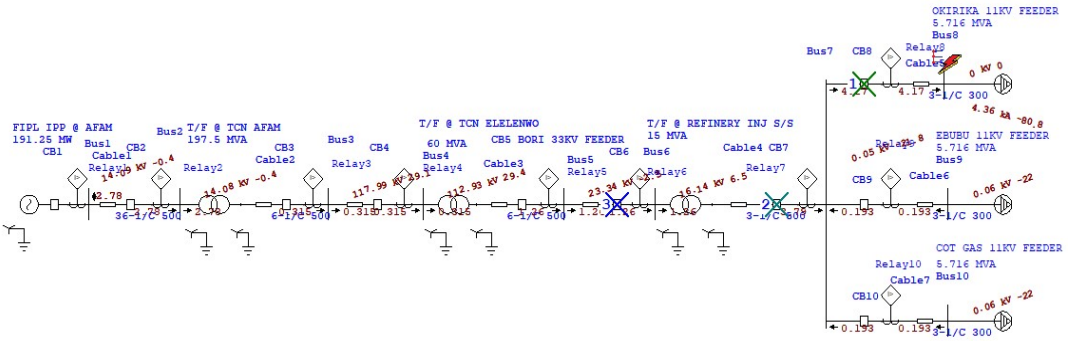

Figure 10: Star Sequence of Operation after 3-Phase Short Circuit Fault Simulation of Bus 8

The SQOP diagram usually display maximum of 3 successive circuit breaker operations in line of defense at any fault occurrence. Fig. 8 displays the star sequence of operation after 3-phase short circuit fault simulation on bus 10 where the Cotgas 11 kV feeder (carrying supply of 300A) radiated from. The circuit breaker number ten (CB 10) responded first to isolate the faulted Cotgas 11 kV feeder followed by CB 7 and then CB 6. The sequence of operation output report will reveal the fault level and actual time of operations of relays and circuit breakers involved in this operation. Both Fig. 9 and Fig. 10 have similar explanation.

Table 4: The sequence of operation events output report 3-Phase (Sym) fault on bus10

Time[ms]	Device	I_F [KA]	T1 [ms]	T2 [ms]	Condition
202	R10	4.171	202		Phase-OC1-51
257	CB10		55.0		Tripped by Relay10 Phase-OC1-51
405	R7	3.786	405		Phase-OC1-51
460	CB7		55.0		Tripped by Relay 7 Phase-OC1-51
2324	R6	1.262	2324		Phase-OC1-51
2376	CB6		52.0		Tripped by Relay 6 Phase-OC1-51

From Table 4 the sequence of operation events output report of the 3-phase (symmetrical) fault on bus 10, relay 10 of CB 10 responded first at 202ms with the short circuit fault current (I_F) of 4.171 kA while circuit breaker number 10 (CB 10) within the zone of protection of R10 operated after 55ms delay of CB response time characteristic (depending of the CB type or make), hence the total time of operation on Phase-OC1-51 is 257ms. The second relay in the line of defense of this particular fault becomes R7 which responded at 405ms (203ms after) with fault current flow of 3.79 kA, while CB 7 within R7 zone of protection tripped after 55ms delay. Therefore the total time of operation is 460ms. The next relay in the sequence of events output report is R6 at 2324ms while CB 6 responded after 52ms each, hence the total time of operation is 2376ms.

The Star TCC view display curves of all components (such as generators, transformers, lines, cables, relays, fuse etc) in power system network (before fault simulation) that will undergo selectivity analysis under faulty situation. Normalized TCC view will display responses of these same curves after fault simulation.

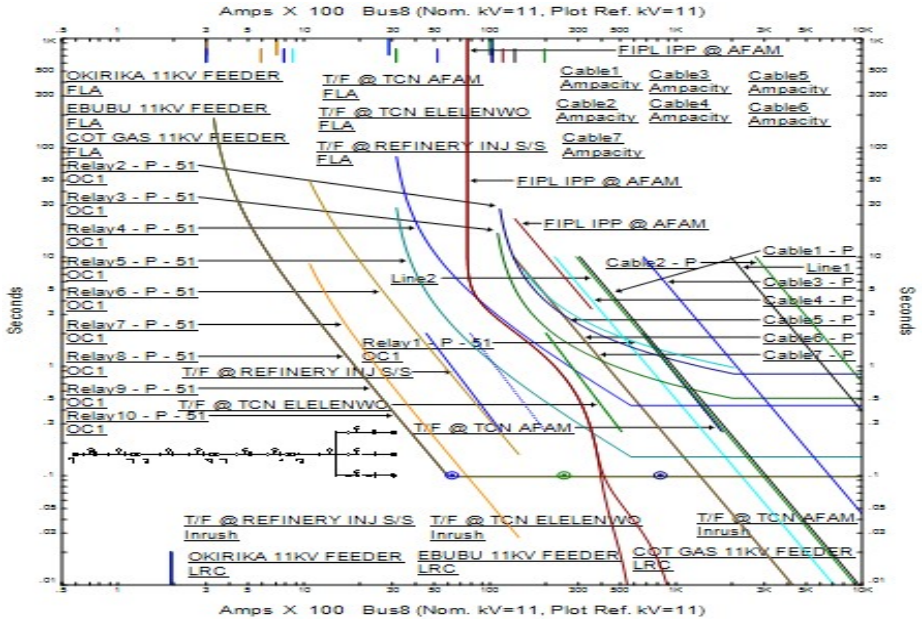

Figure 11: Star TCC view of Network under Study before 3- Phase Fault Simulation

The regular Time Current Curve (TCC) of power system components to undergo the short circuit fault analysis is displayed in Fig.11. These curves are still in ideal condition because no fault simulation has been carried out. Star TCC curves of Relay 6 (R6), R7, R8 and R9 should be to the left of the damage curve of Cable 4 (C4), C5, C6 and C7 in order to ensure that the relay(s) in line of their defense when fault is simulated will operate before reaching the damage curve of components they protect. Therefore, adjustment is unnecessary since the graphical presentation of Star TCC curves in Fig.11 is all in compliance with this rule. It is also a proof that the design of power system components involved in the analysis is in accordance with the required standard.

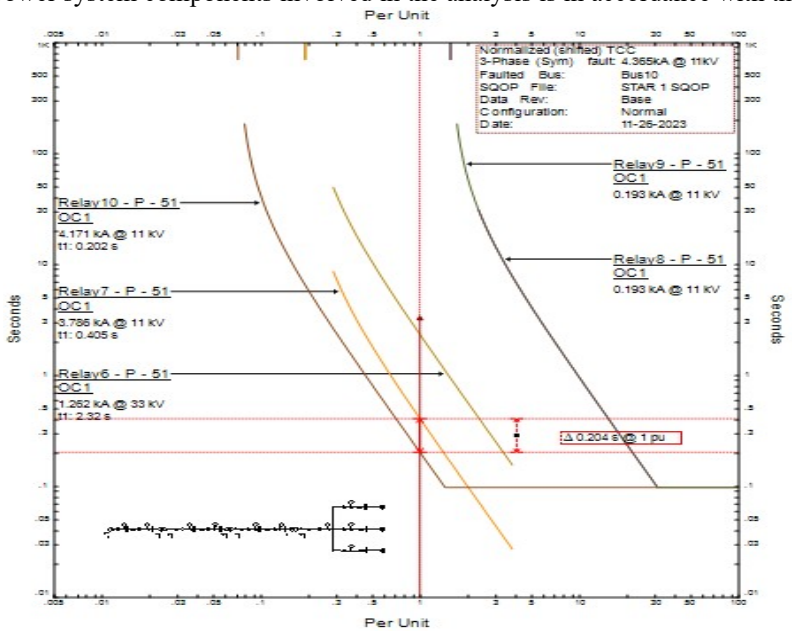

Figure 12:Star Normalized Shifted TCC after 3-Phase Fault Simulation of Bus 10

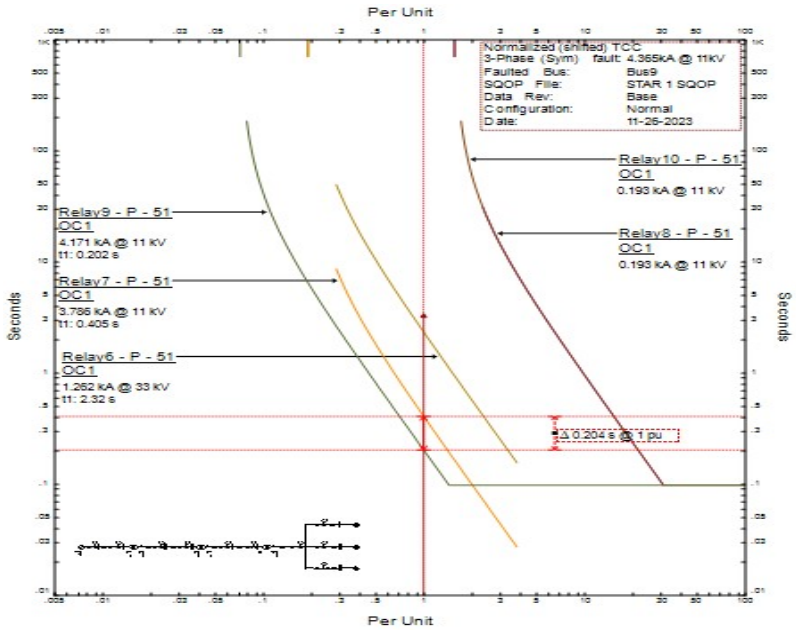

Figure 13: Star Normalized Shifted TCC for 3-Phase Symmetrical Fault at Bus 9

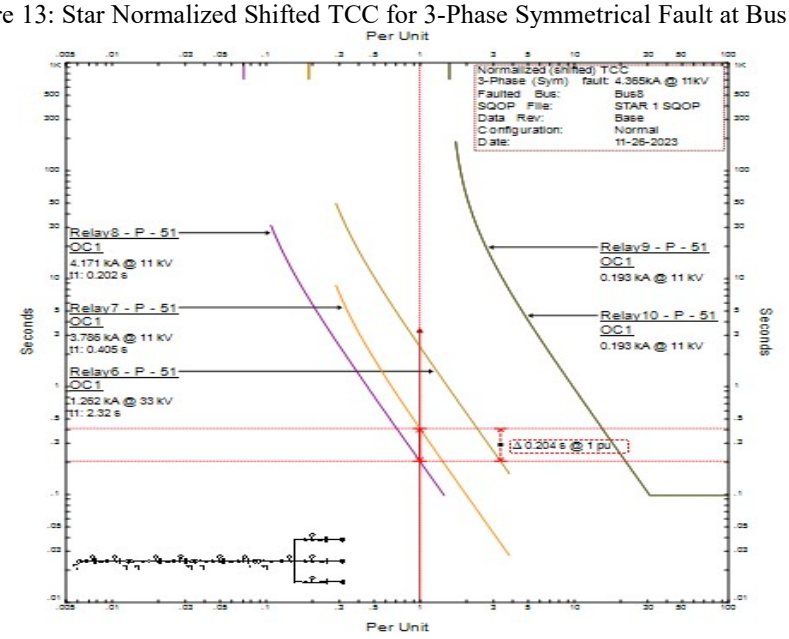

Figure 14: Star Normalized Shifted TCC Curves for 3-Phase Symmetrical Fault at Bus 8

Normalized shifted time current characteristic curves based on the fault current simulation of bus 10 is displayed in Fig.12 and it is the graphical views of calculated fault current flow at each bus upon fault, operating times, corresponding settings, characteristics for a specified fault location and type of all relays featured in Star TCC of Fig.12. Therefore in Fig.12 of normalized time current characteristic display, Relay 10 (R10) operated first with fault current of 4.171 kA and operating time of 202ms, followed by R7 with fault current of 3.786 kA and operating time of 405ms, followed by R6 with fault current of 1.262 kA and operating time of 2.32s. R8 and R9 never operated and they both have the same current contribution which is 0.193 kA. So the two curves are married and represented as one curve. The animation behaviour of R10, R7 and R6 are displayed in both Fig. 11 of star TCC view showing regular time current characteristic curves and Fig. 12 displaying normalized shifted time current characteristic curves of the animated three (3) relays. Again, R7 responded at 204ms (compare with calculated value of 208ms) after R10 operated and this was observed when clicked time difference button was applied on both curves of R10 and R7 and then dragged to 1 pu on the normalized shifted TCC of Fig. 12. Both Fig. 13 and Fig. 14 have the similar explanation.

IV. CONCLUSION

The results of manual calculations are the same with the results obtained using the E-TAP software, hence validating results realized in both II and III. In the analysis carried out on the normalized shifted TCC curves, it is observed that the difference between the operating time of first relay and second relay that responded in line of defence after 3-phase fault simulation in any bus in section III is the same in section II.

The previous relay settings at Refinery injection substation and at Elelenwo transmission substation and at Refinery injection substation created misnomer in the protection system coordination because the symmetrical phase overcurrent fault emanating from any of the three 11KV feeders (Cotgas, Ebubu and Okirika) usually jump and trip Bori 33KV feeder that radiated from Elelenwo transmission substation without arresting this abnormal condition at any of these three 11 kV feeder circuit breakers.

Introduction of new protection settings results gotten after the phase overcurrent coordination using the E-TAP software will cause any of these three 11 kV feeders to trip upon the symmetrical phase overcurrent fault with discrimination, if implemented, and this will end energy loss. The sensitivity of fault clearing time on each feeder will prevent forced interruption of other feeders, reduced voltage, known as voltage dip, loss of energy to earth zero potential, equipment damage, and loss of life, when fault occurs.

The selectivity of each relay in the network under study were demonstrated in all figures of the star sequence of operations with their respective normalized shifted TCC curves after 3-phase symmetrical fault simulation at each bus.

REFERENCES

[1]. Bhuvanesh, A. O, Nirmal- Kumar, C. N, Rashesh, P. M, Vijay, H. M. (2010(a)). Power System Protection and Switchgear: Introduction and Philosophy of a Protective Relaying System. Copyright 2010. Tata McGraw Hill Education Private Limited, 7 west Patel Nagar, New Delhi 110008, pp.1-2.

[2]. Bhuvanesh, A. O, Nirmal- Kumar, C. N, Rashesh, P. M, Vijay, H. M. (2010(b)). Power System Protection and Switchgear: Introduction and Philosophy of a Protective Relaying System. Copyright 2010. Tata McGraw Hill Education Private Limited, 7 west Patel Nagar, New Delhi 110008, pp.7-9.

[3]. PHCN, (2006). Power Holding Company of Nigeria Relaying Protection Course, p1, at professional Skills Training Centre, Kainji, Nigeria , chapter 1, "Principles and Philosophy of Relaying Protection", Introduction, pp 2.

[4]. Kothari D. P and Nagrath I. J (2008(a)). Power System Engineering, Second Edition. Chapter 4, Representation of Power System Components. Copyright 2008. Tata McGraw Hill Education Private Limited, 7 west Patel Nagar, New Delhi 110008, pp.148-149. https://www.academia.edu/104785494/Power_System_Engineering_by_D_P_Kothari_I_G_Nagrath. Date Accessed: 3/21/2024.

[5]. Kothari D. P and Nagrath I. J (2008(b)). Power System Engineering, Second Edition. Chapter 4, Representation of Power System Components. Copyright 2008. Tata McGraw Hill Education Private Limited, 7 west Patel Nagar, New Delhi 110008, pp.453-467. https://www.academia.edu/104785494/Power_System_Engineering_by_D_P_Kothari_I_G_Nagrath. Date Accessed: 3/21/2024.

[6]. SEL,(2020) Tutorial on Symmetrical Components Part 2: Answer Key Ariana Amberg and Alex Rangel, Schweitzer Engineering Laboratories, Inc. https://selinc.com/api/download/100688#:~:text=Because%20a%20three%2Dphase%20fault,positive%2Dsequence%20network%20is%20used. pp 3. Date Accessed: 10/23/2023.

[7]. GEYA,(2022). https://www.geya.net/types-of-overcurrent-relays-and-their-application/. Date Accessed: 3/15/2024.

[8]. Electrical4u,(2019). https://www.electrical4u.net/difference/difference-between-idmt-dt-and-instantaneous-relays/. Date Accessed: 10/23/2023.

[9]. Ram Badri and Vishwakarma D.N, (2011(a)). Power System Protection and Switchgear Second Edition: Chapter4, Fault Analysis. Copyright 2011. Tata McGraw Hill Education Private Limited, 7 west Patel Nagar, New Delhi 110008, pp.18-19. https://gnindia.dronacharya.info/EEE/6thSem/Downloads/POWER-SYSTEMS-II/Books/POWER%20SYSTEMS-II-reference-book-4.pdf. Date Accessed: 3/21/2024.

[10]. Ram Badri and Vishwakarma D.N, (2011(b)). Power System Protection and Switchgear Second Edition: Chapter4, Fault Analysis. Copyright 2011. Tata McGraw Hill Education Private Limited, 7 west Patel Nagar, New Delhi 110008, pp.99-101. https://gnindia.dronacharya.info/EEE/6thSem/Downloads/POWER-SYSTEMS-II/Books/POWER%20SYSTEMS-II-reference-book-4.pdf. Date Accessed: 3/21/2024.

[11]. Ram Badri and Vishwakarma D.N, (2011(c)). Power System Protection and Switchgear Second Edition:Chapter4,Fault Analysis. Copyright 2011. Tata McGraw Hill Education Private Limited, 7 west Patel Nagar, New Delhi 110008, pp.102-139. https://gnindia.dronacharya.info/EEE/6thSem/Downloads/POWER-SYSTEMS-II/Books/POWER%20SYSTEMS-II-reference-book-4.pdf. Date Accessed: 3/21/2024.

[12]. Ram Badri and Vishwakarma D.N, (2011(d)). Power System Protection and Switchgear Second Edition: Chapter 5, Overcurrent Protection. Copyright 2011. Tata McGraw Hill Education Private Limited, 7 west Patel Nagar, New Delhi 110008, pp.221-227. https://gnindia.dronacharya.info/EEE/6thSem/Downloads/POWER-SYSTEMS-II/Books/POWER%20SYSTEMS-II-reference-book-4.pdf. Date Accessed: 3/21/2024

[13]. Ram Badri and Vishwakarma D.N, (2011(e)). Power System Protection and Switchgear Second Edition: Chapter 5, Overcurrent Protection. Copyright 2011. Tata McGraw Hill Education Private Limited, 7 west Patel Nagar, New Delhi 110008, pp.228-233. https://gnindia.dronacharya.info/EEE/6thSem/Downloads/POWER-SYSTEMS-II/Books/POWER%20SYSTEMS-II-reference-book-4.pdf. Date Accessed: 3/21/2024.

[14]. Singh Ravindra .P, (2009). Switchgear and Power System Protection. PHI Learning Private Limited. New Delhi 110001, 2009. Copyright 2009, ISBN-978-81-203-3660-5. Chapter 6, pp. 105-115.

[15]. Murthy, P. S. R, (2007), Power System Analysis: Chapter 6: Short Circuit Analysis. Copyright 2007. BS Publications 4-4-309, Giriraj Lane,Sultan Bazar, Hyderabad - 500 095 A.P. ISBN 978-81-7800-161-6. pp. 178.